

Performance Improvement of the Hybrid Switch Reluctance Motor by Notching Method

Saeed Hasanzadeh^{1*} (Corresponding author), Hossein Rezaei², Hadis Taheri³

*,¹ -Department of Electrical and Computer Engineering, Qom University of Technology, Qom, Iran
(e-mail: hasanzadeh@qut.ac.ir, phone: +98-9127123710)

² - Department of Electrical and Computer Engineering, Babol Noshirvani University of Technology, Babol, Iran & Mazandaran Regional Electric Company, Sari, Iran. (e-mail: hosseinrezaei1367@nit.ac.ir, phone: + 98-9111545092)

³ - Department of Electrical and Computer Engineering, Qom University of Technology, Qom, Iran (e-mail: hadistaheri1997@gmail.com, phone: +98-9198227371)

Abstract- Hybrid switch reluctance motors are the family of switch reluctance motors (SRMs) that attenuate the magnetic saturation and increase the air gap magnetic flux by exploiting permanent magnets. The permanent magnet auxiliary air gap flux can affect the average torque and ripple. Commonly, the torque ripples reduction comes with the average torque drop. In this paper, the torque ripple reduction and average torque improvement are achieved for a 6/10 pole hybrid switch reluctance motor by inserting two symmetrical notches on its rotor. Also, the lengths of magnet and rectangular notches are optimized by the finite element method and sensitivity analysis. The comparison of the optimized design with the initial one carried out by finite element proves the efficiency of the proposed model.

Keywords: Hybrid Switch Reluctance Motor (*HSRM*), *Finite Element Method (FEM)*, *Ripple Torque*, *Average Torque*, *Notching*.

1. INTRODUCTION

Simple structure, fault tolerance, reliability, and robustness due to no winding structure of rotor in switch reluctance motors have attracted particular attention in domestic applications [1-3]. Also, by using PMs, the hybrid SRMs (HSRMs) can develop higher average torque and better starting capability with less-saturated core operation [4-5]. However, the high torque ripple is estimated as a major drawback that limits its applications.

Increasing rotor pole numbers in [5] leads to a higher starting torque, lower high-speed torque, and better torque ripple. Also, the saturation performance, average, and starting torques are improved by adding PMs to SRM. In [6], the laminated stator and rotor topology is proposed to improve average torque and torque ripple using short-flux magnetic paths. However, this design causes the core product to be

complicated. The stator tooth angle, rotor pole arc, and PM thickness are optimized for better torque development and load capability by FEM in the modular-stator HSRM [7-8]. In [9], a Genetic Algorithm (GA) is carried out for optimizing the dimensions of rotor tooth, stator yoke, and stator window with the objective of maximum average torque and minimum torque ripple. The objective function of high starting torque, low torque ripple, and high efficiency are proposed in [10] to optimize the rotor and stator pole arcs and an outer rotor diameter of an HSRM by FEM. Although, in some research, the SRM torque ripple is considered an objective in the optimization, its torque ripple does not resolve and is still high and remains a challenge. In [11], the torque ripple is decreased significantly through notching rotor structure, which strongly impacts the flux harmonics and torque ripple minimization. However, the average torque is also weakened by inserting a single notch into the rotor structure. A notching method is a practical approach inserted on the rotor/stator topology to reduce torque ripple, noise, and power factor [12-13]. Despite its simplicity and effectiveness in improving several performance indexes, this approach is not paid full attention to in most papers that deal with HSRM design and optimization. The reduction of developed torque is another challenge in the notching method. The method presented in this paper can be developed and implemented on linear machines with similar hybrid structures [14-15].

In this paper, the structure of an HSRM is improved by adding two symmetrical notches on the rotor. After that, the PM length and notching span are optimized by FEM in order to improve the average torque in a minimum PM length and torque ripple. The organization of this paper is as follows: In Section 2, the initial design and topology of HSRM are described. Section 3 of the paper deal with the principles and parameters of the design and methods of reducing the proposed motor ripple, such as the longitudinal dimensions of the magnet. Section 4 describes the design of the new rotor structure for the proposed motor. Section 5 presents the results of the simulations, and the final conclusions are made in Section 6.

2. PERMANENT MAGNET-REINFORCED HYBRID SWITCH RELUCTANCE MOTOR

The HSRM topology is depicted in Fig. 1. The initial design parameters of the hybrid reluctance switch motor are selected based on reference [9] and listed in Table 1. The initial design consists of 6 stator poles, and 10 rotor poles with permanent magnets (PMs) adjusted adjacent to the stator pole. The operation of the HSRM is based on the use of a PM. The function of the magnets attenuates the magnetic saturation at the stator pole and increases the magnetic flux in the air gap, which can significantly increase the output torque. The HSRM magnetic equivalent circuit is symmetrical, and the magnetic excitation (MMF) is provided by the magnet and the field current in each phase. The operation of the magnetic core at the knee point of the B-H curve causes the nonlinear behavior of the HSRMs, creating harmonics and torque ripple, consequently.

3. OPTIMIZED DESIGN

In this section, the design improvement and optimization are carried out to mitigate the torque performance. As so, two symmetrical notches are inserted on the rotor, and to evaluate the ripple performance and average torque, the impact of PM length and notch dimensions are analyzed by FEM sensitivity analysis. Fig. 2 shows a modified design by creating notches in rotor poles with the notching method.

3.1. Notch creation on the rotor

In the HSRM, magnetic torque is produced by the interaction of rotor parts and stator teeth. The internal gravitational force between the teeth and the motor poles tries to maintain a balance between the stator teeth and the rotor sections; to reduce this equilibrium, it is necessary to minimize the effect of harmonic flux changes on the air gap.

Creating symmetrical, small, and smooth notches at the end of rotor poles reduce the harmonic distortion of air-gap flux and torque ripple. On the other hand, the developed torque is decreased due to an increase in the effective air gap and flux weakening. Therefore, the average torque should be observed in addition to investigating the impact of notches on the torque ripple. To this end, the notch height and number should be carefully selected in order to avoid the average torque drop. Two symmetrical notches with 2 mm height are inserted at each rotor pole since a structure with more than two notches and 2 mm height causes a significant reduction in the average torque. Also, the optimum notching span will be found via sensitivity analysis. According to Fig. 3, two rectangular notches are inserted symmetrically at the end of rotor poles to reduce air-gap flux and torque ripple harmonics. The notching span α_n can be derived as a function of notching height h_n , efficiency η and rotor radius R_1 .

$$\alpha_n = \eta \frac{h_n}{R_1} \quad (1)$$

In the proposed model, the notching span α_n varies between 0 and 1 with a step of 0.1, and the size of notching height h_n is fixed at the value of 2 mm. Harmonic distortion of air-gap flux is managed by selecting the correct notching span value, which reduces torque ripple.

However, like other common methods for torque ripple reduction, the notching method reduces torque ripple and average torque, which is not optimal. Therefore, it is necessary to check the magnetic part to compensate for the average torque reduction. For this purpose, the optimum PM length can be selected by considering the torque ripple, average torque, and PM cost.

3.2. The Effect of PM Length on Average Torque

Like the electromagnet coil, the PMs create Magnetomotive force proportional to their length and magnetization (magnetization length) in which the developed magnetic flux passes through various air paths. As a consequence, the flux density increases by increasing magnetization length. On the other side, as the length of magnetization increases, the PM flux closes in the longer air gap paths and is weak, reducing the developed torque. Therefore, an excessive increase of PM magnetization length can deteriorate torque performance. As depicted in Fig. 4 and Table 2, in the notchless rotor structure, increasing the PM length reduces the torque ripple significantly

while the average torque does not increase necessarily. Therefore, there is an optimum PM length for each rotor structure. The following section evaluates the torque performance in different notching spans and PM lengths via FEM. As listed in Table 3, the PM length varies between 5 to 10 millimeters in models I1 to I6. In each model, the notching span changes from 0 to 1 with the step of 0.1 while the notching height is constant. As a result, the optimum PM length and notching span can be derived. The developed torque versus PM length is illustrated in Fig. 4. Also, the average torque, torque ripple, and variations percentage compared to the initial design are also written in Table 2.

4. SIMULATION RESULTS

In this section, the HSRM performance is analyzed to evaluate and compare torque ripple and average torque in different magnet lengths and notching spans at a rotational speed of 1000 rpm and a field current of 20 amperes with FEM simulations. The flux lines and their spectrum are also drawn in Fig. 5. The specifications of the finite element model are listed in Table 4.

This sensitivity analysis aims to find the appropriate rotor notch and PM length values to achieve a minimum torque ripple in an acceptable average torque; as stated in the previous section, six different modes are designed, applied, and simulated on the initial design. The variations of average torque and torque ripple are derived through FEM with respect to notching spans in different PM lengths and are illustrated in Fig. 6 and Fig. 7. In model I1, the PM length is 5 mm, and the range of notching span varies between 0 to 1 mm with a ratio of 0.1. According to Fig. 6 and Fig. 7, the torque ripple and average torque decrease in the same way. However, the torque ripple is intensified when the notching span varies from 0.1 to 0.2 mm.

The results show that compared to the initial model, the torque ripple and average torque are reduced up to 13.9% and 1.6%, respectively. In other words, a larger notching span leads to having a more significant impact on ripple reduction. In Model I2, the magnet length was considered to be 6 mm. increasing the

magnet length positively affects improving the objectives of average torque and ripple. As seen in Figs 6 and 7, increasing PM length does not necessarily strengthen the average torque. This mainly occurs from 9 to 10 millimeters PM length, in which the average torque is weakened in all notching spans. Although increasing the PM length strengthens the magnetic flux and developed torque due to magnetic MMF amplification, the magnetic reluctance is increased at high PM lengths. It attenuates the flux field and output torque. Therefore, the PM length always reduces the torque ripple but does not always increase the average torque.

5. OPTIMUM DESIGNS OF HSRM

This paper defines the objective function based on achieving maximum average torque minimum torque ripple and considering the PM cost by placing PM length into the function. As so, the objective function is defined as:

$$Cost - Function = (a \times T_{ave} + b \times Ripple) \frac{PM_Length}{100} \quad (2)$$

where T_{ave} is the average torque, the "a" coefficient should be negative to minimize the cost function, whereas the "b" coefficient has a positive value. These coefficients are selected depending on the designer's emphasis. The design variables are PM length and notch dimensions. In equation (2), the other design parameters, such as air gap PM thickness, are assumed to be constant. The definition of the cost function is entirely a matter of taste, and we define it in such a way as to emphasize the main goal, which is to increase the average torque and decrease the ripple in a minimum PM cost.

This function shows that the lower the torque ripple and the higher the average torque, the smaller the numerical value of the target function in a defined and limited PM length. The optimum designs yielding minimum cost functions are attained, as shown in Fig. 8. As written in Table 5, in addition to torque performance, the back-emf total harmonic distortion (back-emf THD) and power factor are improved in the optimum designs. Although the HSRM material cost increases with the PM length in the optimum designs, a remarkable improvement in the torque ripple and average torque makes them financially reasonable.

The first optimum design is calculated with an emphasis on the average torque (-0.25, 0.75). It is shown that there is a 9.77% development in the average torque and 66.3% improvement in the torque ripple. Also, there is another improvement in THD and PF by 6.5% and 6.3 % compared to the initial state. Comparisons of developed torque in the optimum designs with the initial notchless topology are illustrated in Fig. 9. Due to improvement in average torque, torque ripple, THD, and PF, this motor is significantly optimized. By selecting the weighting factors to (-0.3, 0.7) in the (2) cost function, the second optimum design is obtained with a magnet length of 8 mm and a notching span of 0.9 mm. In this design, a 63.6%

reduction in the torque ripple and a 7.2% increase in the average torque have occurred. Improving the THD and PF is also achieved to 5.4% and 6.05%, respectively.

Table 5 shows that although the second design has less improvement than the first design in average torque and ripple, a 20% saving in the PM consumption is observed. Since its performance is close to the first design, this optimum point can be a desired alternative for low-cost applications. Also, in Table 5, the optimum designs may be compared with the experimental results obtained in [9]. As can be observed, the experimental set-up in [9] offers better average torque during severe torque ripple. The first optimum point reaches 89.5% of T_{ave} value in [9] and 64% improvement in torque ripple by consuming 100% more magnets. The average torque reaches 87.4% of T_{ave} in [9] for the second optimum design, while a 61.5% reduction in torque ripple with 60% more PM consumption than the PM in [9].

6. CONCLUSION

In this paper, optimum designs of a 6/10 pole hybrid switch reluctance motor are presented, which optimizes the notching span of the rotor and PM length to improve its performance. Different notching spans and PM lengths were investigated. Finally, two optimum designs are obtained based on the cost function satisfying torque ripple and average torque in the minimum additional PM cost. The proposed model with a notching span of 0.4 mm and a PM length of 10 mm has been selected as the first optimum design. Compared to the notchless initial model, the torque ripple is improved by 66.3%, while the average torque is enhanced by 9.8%. In the second design with more emphasis on torque ripple, these improving percentages are 63.6% and 7.2% for torque ripple and average torque, saving 20% in PM cost. Also, the proposed optimum designs decrease harmonic distortion and strengthen the power factor.

7. REFERENCES

- [1] Bartolo, J.B., Degano, M., Espina, J., *et al.* “Design and initial testing of a high-speed 45-kW switched reluctance drive for aerospace application”, *IEEE Trans. Ind. Electron.*, 64(2), pp. 988–997 (2017).
- [2] Bostanci, E., Moallem, M., Parsapour, A., *et al.* “Opportunities and challenges of switched reluctance motor drives for electric propulsion: A comparative study”, *IEEE Trans. Transp. Electrifi.*, 3(1), pp. 58–75 (2017).
- [3] Naseh, M., Hasanzadeh, S., Dehghan, *et al.* “Optimized design of rotor barriers in pm-assisted synchronous reluctance machines with taguchi method”, *IEEE Access*, 10, 38165–38173 (2022).
- [4] Ding, W., Hu, Y., Wang, T., *et al.* “Comprehensive research of modular E-core stator hybrid-flux switched reluctance motors with segmented and nonsegmented rotors”, *IEEE Trans. Energy Convers.*, 32(1), pp. 382–393 (2017).
- [5] Ding, W., Yang, S. and Hu, Y. “Development and investigation on segmented-stator hybrid-excitation switched reluctance machines with different rotor pole numbers”, *IEEE Trans. Ind. Electron.*, 65(5), pp. 3784–3794 (2018).

- [6] Ding, W., Yang, S., Hu, Y., *et al.* “Design consideration and evaluation of a 12/8 high-torque modular-stator hybrid excitation switched reluctance machine for EV applications”, *IEEE Trans. Ind. Electron.*, 64(12), pp. 9221–9232 (2017).
- [7] Shirali, E., Hasanzadeh, S. and Dehghan, S.M. “FEM-aided analytical model and control of SSLFSM thrust force”, *Comput. Intell. Electr. Eng.*, 11(2), pp. 87–94 (2020).
- [8] Mousavi-Aghdam, S.R., Feyzi, M.R., Bianchi, N., *et al.* “Design and analysis of a novel high-torque stator-segmented SRM”, *IEEE Trans. Ind. Electron.*, 63(3), pp. 1458–1466 (2016).
- [9] Zhu, J., Cheng, K.W.E. and Xue, X. “Design and analysis of a new enhanced torque hybrid switched reluctance motor”, *IEEE Trans. Energy Convers.*, 33(33), pp. 1965–1977 (2018).
- [10] Diao, K., Sun, X., Lei, G., *et al.* “Multimode optimization of switched reluctance machines in hybrid electric vehicles”, *IEEE Trans. Energy Convers.*, 36, 2217–2226 (2021).
- [11] Mehta, S., Kabir, M.A., Pramod, P., *et al.* “Segmented Rotor Mutually Coupled Switched Reluctance Machine for Low Torque Ripple Applications”, *IEEE Trans. Ind. Appl.*, 57(4), pp. 3582–3594 (2021).
- [12] Xiang, Z., Quan, L. and Zhu, X. “A new partitioned-rotor flux-switching permanent magnet motor with high torque density and improved magnet utilization”, *IEEE Trans. Appl. Supercond.*, 26(4), pp. 1–5 (2016).
- [13] Sikder, C., Husain, I. and Ouyang, W. “Cogging torque reduction in flux-switching permanent-magnet machines by rotor pole shaping”, *IEEE Trans. Ind. Appl.*, 51(5), pp. 3609–3619 (2015).
- [14] Esfahanian, H.R., Hasanzadeh, S., Heydari, M., *et al.* “Design, Optimization, and Control of a Linear Tubular Machine Integrated with Levitation and Guidance for Maglev Applications”, *Sci. Iran.*, (2021).
- [15] Hasanzadeh, S., Rezaei, H. and Qiyassi, E. “Analysis and optimization of permanent magnet dimensions in electrodynamic suspension systems”, *J. Electr. Eng. Technol.*, 13(1), pp. 307–314 (2018).

List of Captions:

* Figure Captions:

Fig. 1. The initial design of HSRM

Fig. 2. A modified design by creating notches in rotor pole with notching method

Fig. 3. Notch design model and parameter

Fig. 4. Developed torque vs. rotor position in various PM lengths for notchless rotor structure

Fig. 5. Flux lines and flux density spectrum

Fig. 6. Variations of average torque versus notching span in various PM lengths

Fig. 7. Variations of torque ripple versus notching span in various PM lengths

Fig. 8. (a) First, (b) Second optimum designs of HSRM (PM length and notching span)

Fig. 9. Developed torque vs. rotor position in initial and optimum designs

*Table Captions:

Table 1. Design Parameters of HSRM

Table 2. Average torque and torque ripple vs. PM length in notchless rotor structure

Table 3. Motor models with different PM lengths and notching spans

Table 4. Finite element specifications

Table 5. Optimum designs of HSRM (PM length and notching span)

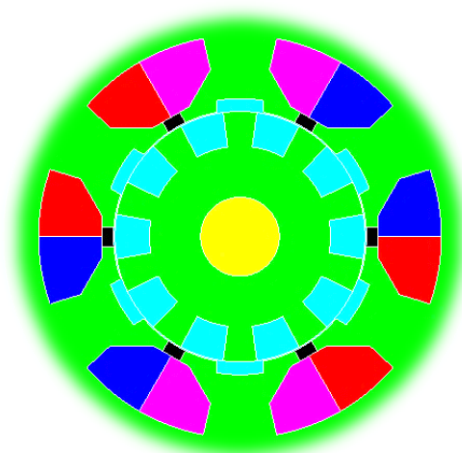


Fig. 1. The initial design of HSRM

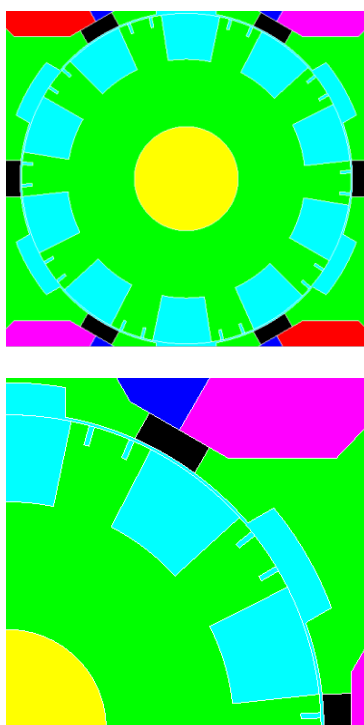


Fig. 2. A modified design by creating notches in rotor pole with notching method

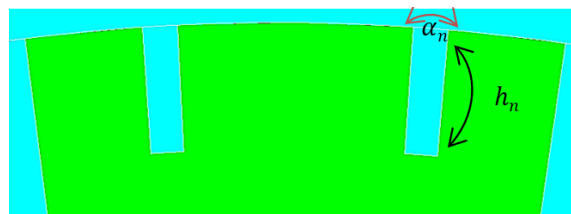


Fig. 3. Notch design model and parameter

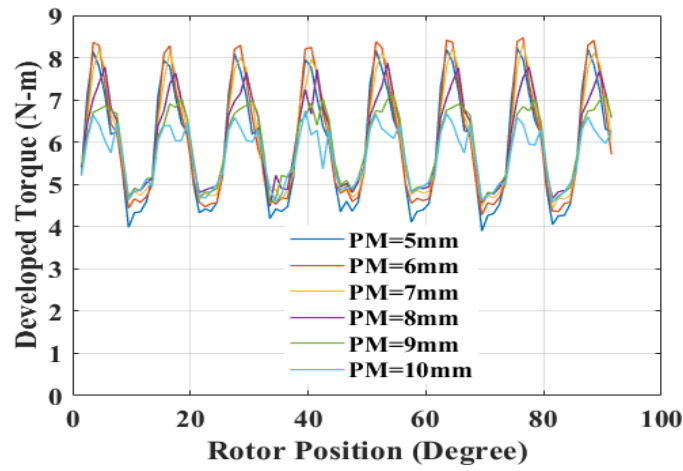


Fig. 4. Developed torque vs. rotor position in various PM lengths for notchless rotor structure

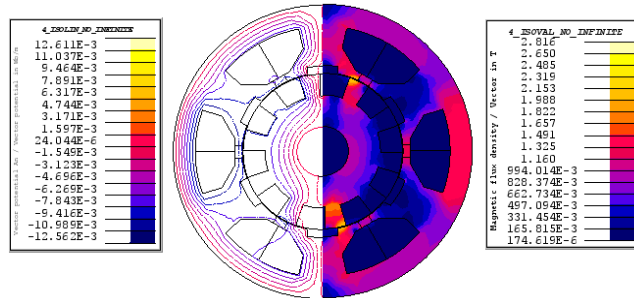


Fig. 5. Flux lines and flux density spectrum

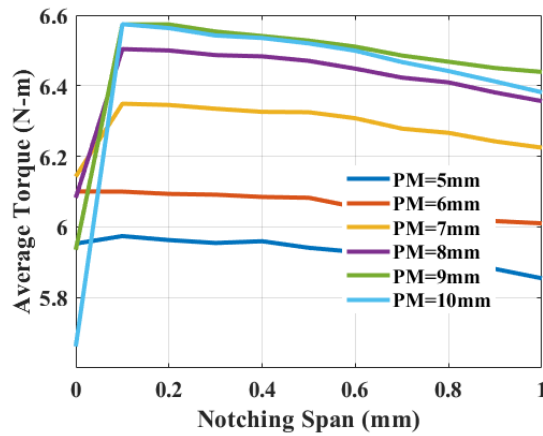


Fig. 6. Variations of average torque versus notching span in various PM lengths

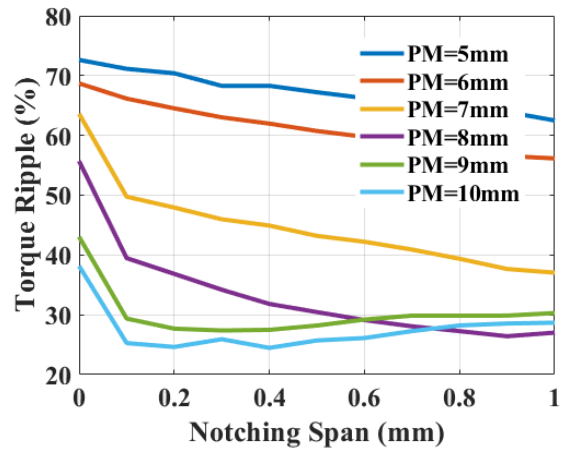
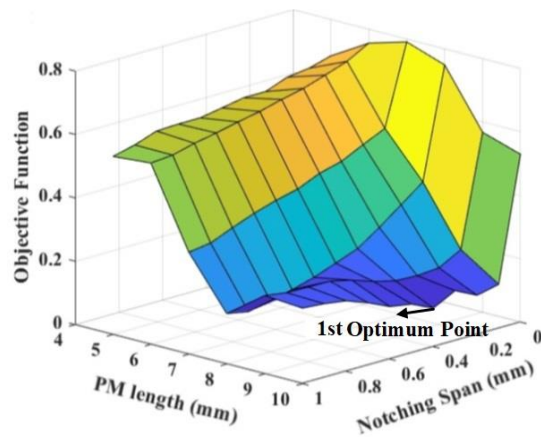
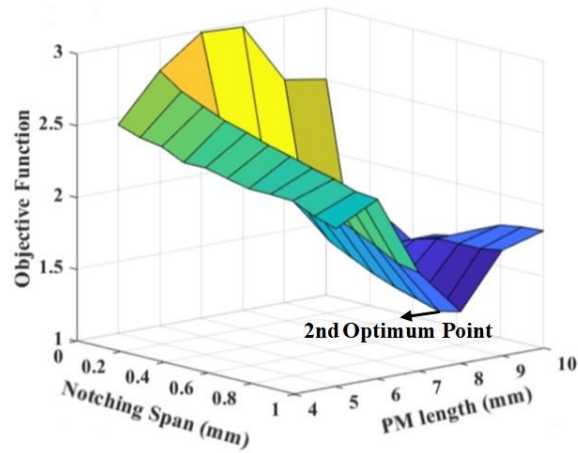


Fig. 7. Variations of torque ripple versus notching span in various PM lengths



(a)



(b)

Fig. 8. (a) First, (b) Second optimum designs of HSRM (PM length and notching span)

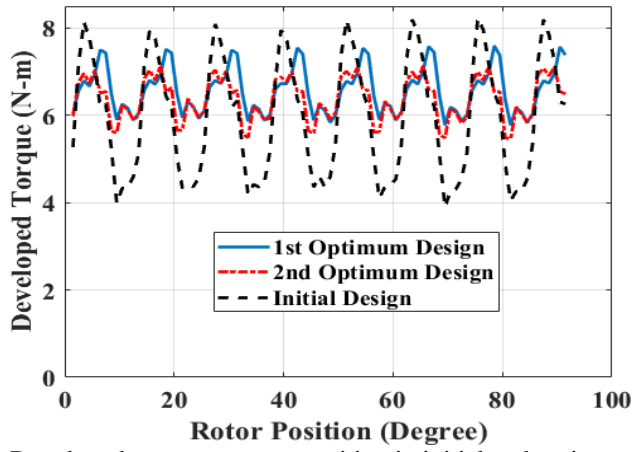


Fig. 9. Developed torque vs. rotor position in initial and optimum designs

Table 1. Design Parameters of HSRM

Outer diameter of the stator (mm)	120
Air gap (mm)	0.3
Phase	3
Number of coils	140
PM Thickness (mm)	3
Rotor diameter (mm)	63.7
Power (watts)	770
Speed (rpm)	1000

Table 2. Average torque and torque ripple vs. PM length in notchless rotor structure

PM length (NdFeB)	Average torque (N-m)	Variation of Tave decrease (-) increase (+)	Torque ripple (%)	Variation of ripple decrease (-) increase (+)
Initial design PM=5mm	5.95	0%	72.62	0%
PM=6mm	6.1004	+2.48%	68.69	-5.41%
PM=7mm	6.142	+3.18%	63.6	-12.41%
PM=8mm	6.082	+2.178%	55.69	-23.31%
PM=9mm	5.935	-0.296%	43.29	-40.74%
PM=10mm	5.661	-4.89%	38.15	-47.46%

Table 3. Motor models with different PM lengths and notching spans

Model	PM Length (mm)	Notching Span	Notching Height (mm)
I1	5	Range 0 to 1 with a ratio of 0.1	2
I2	6	Range 0 to 1 with a ratio of 0.1	2
I3	7	Range 0 to 1 with a ratio of 0.1	2
I4	8	Range 0 to 1 with a ratio of 0.1	2
I5	9	Range 0 to 1 with a ratio of 0.1	2
I6	10	Range 0 to 1 with a ratio of 0.1	2

Table 4. Finite element specifications

Timestep	0 to 0.015 (1.67e-4 Sec)
Solution type	Transient
	14549 nodes
Mesh information	1523 line elements
	7244 surface elements

Table 5. Optimum designs of HSRM (PM length and notching span)

	PM length	Span	T_{ave} (N-m)	Ripple (%)	Back-emf THD (%)	PF (%)	Factors
Initial Design	5 mm	0	5.95	72.6	56.6	0.413	-
1st Optimal Design	10 mm	0.4	6.54 (+9.8%)	24.5 % (-66.3%)	52.9 (-6.5%)	0.439 (+6.3%)	a = -0.75 b = 0.25
2nd Optimal Design	8 mm	0.9	6.38 (+7.2%)	26.4 % (-63.6%)	53.5 (-5.4%)	0.438 (+6.1%)	a = -0.3 b = 0.7
Experimental results in [9]	5 mm	0	7.3	68.5 %	-	-	-

Biographies:

Saeed Hasanzadeh received the M.Sc. and Ph.D. degrees in electrical engineering from the University of Tehran (UT), Tehran, Iran, in 2006 and 2012, respectively. His M.Sc. thesis and Ph.D. dissertation have been conducted in the field of high voltage engineering and wireless power transfer (WPT), respectively. In 2013, he joined the Department of Electrical and Computer Engineering, Qom University of Technology, as an Assistant Professor. He was recognized as an Outstanding Lecturer with the Qom University of Technology, in 2020. He is currently the Dean of the Department of Electrical and Computer Engineering (ECE), Qom University of Technology. His current research interests include power electronics, electrical machines, wireless power transfer, and high-voltage engineering. He is a TPC Member of the IEEE Power Electronics & Drives: Systems and Technologies Conference (PEDSTC). He was a recipient of the Top Research Prize of the Qom University of Technology in 2019. He is an Editorial Board of the Power Electronics Society of Iran (PELSI).

Hossein Rezaei received the B.S. degree in electrical engineering from Shahid Beheshti University, Tehran, Iran, in 2011, and the M.Sc. degree in electrical engineering from the University of Tehran, Iran, in 2013. He is currently pursuing the Ph.D. degree in electrical engineering with the Babol Noshirvani University of Technology, Iran. His research interests include hybrid and electrical vehicles, electrical machines, and power electronics.

Hadis Taheri received the B.S. degree in electrical engineering from Buein Zahra Technical University, Buein Zahra, Iran, in 2019, and the M.Sc. degree in electrical engineering from the Qom University of Technology, Qom, in 2021. Her research interests include power electronics and electrical machines.